Mechanics & Industry **21**, 307 (2020)
© AFM, EDP Sciences 2020
https://doi.org/10.1051/meca/2020015

Mechanics & Industry

Available online at:
www.mechanics-industry.org

Regular Article

Experimental investigation into characterization and machining of Al + SiCp nano-composites using coated carbide tool

Pradyut Kumar Swain[1,*], Kasinath Das Mohapatra[1], Ratnakar Das[2], Ashok Kumar Sahoo[3], and Amlana Panda[3]

[1] Department of Mechanical Engineering, NMIET, BBSR, Odisha, India
[2] Department of Manufacturing Engineering, NIFFT Ranchi, India
[3] Department of Mechanical Engineering, KIIT Deemed to be University, Odisha, Bhubaneswar, India

Received: 1 August 2019 / Accepted: 18 February 2020

Abstract. The current research paper discusses the characterization and machining (turning) operation of aluminium (Al) and silicon carbide nano particle (SiCp) nano composite. The paper reveals proper distribution of silicon carbide nano particles (25nm) with aluminium metal matrix. Initially, tensile test has been carried on metal matrix nano composite to study its different properties. It was noticed that the properties of Al-SiCp increases by increasing the weight percentage of SiCp. Viker hardness test has also been conducted to find out the hardness of metal matrix nano composites. Different techniques i.e. Optical microscopy EDX-Analysis were utilized to find out various ingredients of the nano-composite material. The experimental study was carried out using Taguchi L_{16} orthogonal array by taking three different factors at four different levels each. The response parameters i.e. flank wear of coated carbide insert and surface roughness of Al-SiCp has been optimized by using Principal Component Analysis (PCA). Various graphs like main effect plot and normal probability plot have been plotted and studied properly. Different optical images of coated insert carbide tools (Insert CNMG 12040822TN 6010) at different runs were conducted to visualize the effects of process and response parameters. From the ANOVA table, it was found that cutting speed as well as depth of cut are found to the most vital parameters in influencing the responses for VBc and depth of cut and feed are found to the most significant parameters in influencing the responses for Ra.

Keywords: Flank wear / tensile test / surface roughness / depth of cut / principal component analysis

1 Introduction

The metal matrix nano composites and its applications are increasing in day today's life in both automobile and aerospace industries because of their improved properties. Now a days the people demand for innovative and new technologies products to sustain in the global economy. Excellent high strength to weight ratio, higher mechanical and physical properties has led to a better interest and demand in different industries of various materials in which saving of material is a critical issue. At present, various MMCs are synthesized among which Al-SiCp has emerged for a variety of special and general applications. Moreover, Aluminium matrix composites have been widespread its applications and uses due to its high wear resistance and low cost. Metal matrix nano composites recently gained its popularity due to change in its physical properties i.e. thermal expansion, thermal diffusivity, density and mechanical properties i.e. tribological behavior, tensile, compressive behavior, creep, etc. by changing the filler phase. In Al-SiCp,, aluminum alloys are mostly used due to its low density, excellent corrosion resistance, good electrical and thermal conductivities, high temperature applications, desired dimensional accuracy and high damping capacity. Almost in every industry, Al metal matrix composites will be the essential material which satisfies the requirements i.e. high strength, thermal conductivity, low density and good damping properties [1]. MMC exerts better mechanical properties as compared to alloys with respect to its stiffness and high strength to weight ratio for aerospace and various automobile applications. In MMNC's, the reaction takes place in between the reinforcement particulate and metal matrix that can change the interface and arrangement of the matrix leading to interfacial compounds. These inter metallic compounds produce harmful effects to the mechanical properties and also beneficial effects in improving the ductility and toughness of the nano composites. The SiCp acts as a fiber reinforced to Al metal matrix composite (Al-SiCp) which is considered as a suitable and favorable type of MMC's [2]. Al-SiCp

* email: pradyutkumarswain26@gmail.com

composites have been useful in various engineering fields i.e. in structural and functional applications due to change in the mechanical properties depending upon the proportion of chemical and reinforcement composition of Al matrix [3]. SiCp particles can improve the yield stress and Young's modulus of Al-SiCp nano composite material but, the fracture toughness and ductility of the composite is considerable worse than wrought alloys. Nano-composites offers good thermal, tribological and mechanical properties over micro-composites [4]. Therefore, the developed nano-composite materials have been employed as a substitute material to solve the above drawbacks.

2 Literature review

Different observations and literature surveys have been made by different researchers in the field of Al-SiCp nano particles nano matrix composites and their contributions have been mentioned and listed below. Kolo et al. [5] investigated the planetary milling for nano-SiCp reinforced Al MMC. It was concluded that there was a significant effect on hardness of hot compacted samples and powder morphology on selection of the process control agent. Gopalakannan and Senthivelan [6] studied machining of aluminium silicon carbide nano-composites and its application by response surface method. A mathematical model was formulated to estimate the machining characteristics. It was found that pulse current was an important factor in affecting the output responses i.e. MRR, EWR and surface roughness. The nano-sized SiCp reinforced commercial casting of Al alloy matrix was experimented and evaluated by Mazahery and Shabani [7]. Li et al. [8] studied the improved and fabrication and mechanical behaviour of SiCp particles for carbon nanotubes which was reinforced by 6061 Al MMC. Commercial casting of Al-SiCp nano composite material was produced where SiCp works as reinforcement. A methodology study was also proposed to investigate for SiCp reinforced commercial casting Al alloy matrix which was based on Artificial Neural Network (ANN) analysis and Finite Element Method (FEM). It was observed that these methods were capable of producing a small amount of information for complex relationships and estimated solutions. While, Chawla and Shen [9] studied the mechanical behaviour of the reinforced particles of metal matrix composites, Dhanashekar and Kumar [10] focussed on the squeeze casting of metal matrix (Al) composites. The tribological behaviour of Al hybrid MMC was studied by Padmavathi and Ramakrishnan [11]. Their investigations focussed on wear as well as friction properties of Al6061 matrix with SiCp reinforcement particle and various volume fraction of Multiwall carbon nanotube. For this investigation stir casting was used. Composite materials were analysed and studied and it was found that these materials exhibit very less friction coefficient and wear rate as compared to aluminium metal matrix under normal conditions. Koli et al. [12] reviewed the behaviour, properties and methods for Al_2O_3 composites. It was reported that for aluminium alloy, the mechanical properties will be improved when the nano-alumina particles are added up to maximum 4 percentage volume. The impact of nano particles of aluminium based MMC on fatigue strength for aerospace was studied by Divagar et al. [13]. It was investigated that the fatigue life of nano composites material influenced the reinforced nano particles in a fatigue testing machine by means of rotation beam. The integrity of MMNC was also examined by using Scanning Electron Microscopy and Optical Microscopy. It was observed that MMNC consists of AA7075-T651 + SiCp-10% + Al_2O_3-5% ingredient and gives a fatigue strength which is 12.13% more than other composites and base metals. Lijay et al. [14] investigated the characterization of microstructure and mechanical properties of AA6061/TiC Al matrix composites. The composites were synthesized by in situ reaction of potassium fluotitanate and SiCp particle. The microstructures of these produced AMCs discovered a proper distribution of TiC with good bonding and fine interface. Radha and Vijayakumar [15] investigated the wear as well as mechanical properties of AA6061 which were reinforced with grapheme nano-particles particulate composites and silicon carbide. AA6061 reinforced with SiCp (10% of AA) were fabricated by changing the wt.% of graphene (0%, 0.3%, 0.5%, and 0.7%) by using Stir Casting. Their analysis disclosed that the mechanical properties of the workpiece can be improved significantly as compared to Al is reinforced with SiCp particle by addition of graphene. Sijo and Jayadevan [16] investigated and also reviewed the stir cast Al-SiCp metal matrix composite. Different merits of stir casting method were explained by them as compared to other methods. The wear mechanisms and performance of novel boron nitride based tools and super-hard diamond in machining Al-SiCp MMC was investigated by Dhaneswara et al. [17] in which the behavioural studies of SiCp nano particle reinforced Al A356 with Sr-modifier was synthesised by the method of stir casting. Their results concluded that nano composite material achieved its ultimate tensile strength of 176.1MPa and elongation of 6.92% by the addition of 0.25% of SiCp nano particle. The surface behaviour and tribological property of reinforced aluminium matrix nano-composite was studied by Manivannan et al. [18]. Their investigations revealed that the wear characteristics of Al alloy Al 6061 and its nano-composite Al 6061/nano-Silicon carbide were processed by a method of Liquid metallurgy. Reddy et al. [19] studied the SiCp reinforced Al metal matrix nano composites. Their micro-structural assessment showed unvarying distribution of nano SiCp in the MMC as well as robust bonding in between the particle and matrix at the interface. Rana et al. [20] optimized the mechanical properties of AA5083 silicon carbide nano composites material by the application of DOE (Design of Experiment). The effect of process parameters was tested on the outputs. ANOVA test and Fisher's (F-test) were carried out and it was found that the optimal values of the parameters obtained in hardness of the specimen was 2 wt.% of SiCp nano particle whereas the casting temperature was 760 °C and stirrer speed was 550 RPM. Razavi et al. [21] developed a new method of spark plasma sintering and studied the production of Al_2O_3–SiC nano-composites. Their findings showed that the samples containing small sized SiCp have significant effects on hardness, bulk density and strength. Davidson

and Regener [22] compared the aluminium based MMCs reinforced with uncoated and coated particulate SiCp. The effect of techniques of Al MMC properties reinforced with nano Ni-coated Silicon carbide was studied by Abolkassem et al. [23]. To prepare the composites they used three different types of sintering techniques. Their test results revealed that highest densification values (97–100%) was observed on hot pressed samples, followed by HIP samples (94–98%). Chen et al. [24] investigated the mechanism of hybrid Al MMCs and hot deformation behaviour reinforced with nano-TiB_2 and micro-Silicon carbide. Xavior and Kumar [25] reviewed the machinability of hybrid MMC. Ramesh et al. [26] analysed and found the mechanical behaviour and wear properties of Al-SiCp nano composites. Coated and uncoated particulate SiCp were also studied by them on aluminium alloys. Different tests were conducted by them to evaluate the performance of the composite. It was concluded that the reason for increasing porosity and density was due to addition of SiCp. The effect of SiCp reinforcement on the mechanical and physical properties of Al- MMC was investigated by Mohanavel et al. [27]. Influence of additional SiCp were focussed by them which increases the properties of the AA6351 AlMC by the method of liquid metallurgy route. Hardness properties, yield strength, density and impact strength of Al-SiCp were investigated. Their outcomes revealed that Al metal matrix composite increases its mechanical properties by increasing the SiCp particle. Zhang et al. [28] analysed the synergistic-strengthening efficiency and microstructure of CNTs-SiCp by using two nano reinforcements in Aluminium metal matrix composites. The reinforcements of silicon carbide particle (SiCp) and carbon nano-tubes (CNTs) were investigated by them in CNTs-SiCp reinforced Aluminium Matrix Nano-Composites (AMNC). It was concluded that the silicon carbide particles could be used as a ball milling medium when SiCp and CNTs were properly distributed in the Aluminium metal matrix. Shukla et al. [29] reviewed the characteristic behaviour of Al MMC's. Their findings concluded that the SiCp content distribution is partly similar. Further with the increase of SiCp in the Al metal matrix, hardness and tensile strength of AMCs were increased as compared to unreinforced particle when added to the aluminium matrix. Somasundaram et al. [30] experimentally investigated the mechanical properties and roundness error in friction drilling of Al-SiCp metal matrix composites. Their results showed that the hardness and tensile strength increases with the increase in the weight percentage of SiCp particles. Grigoriev and Vereshchaka [31] studied the methodology of formation of multilayer coatings for carbide cutting tools. Similarly, Gangil et al. [32] studied the influence of shoulder geometries and tool pin on microstructure of friction stir processed AA6063/SiC composites. Behera et al. [33] studied the machining operation of Al-SiCp MMCs. Uncoated tungsten carbide was selected as the tool material by them. The effect of response parameters like cutting force and surface roughness on the machinability of LM6/SiCp MMCs at various weight percentages of SiCp were studied. Their findings concluded that the cutting forces and surface roughness (Ra) were affected by depth of cut and cutting speed at fixed feed rate during dry turning operations of MMCs. Loto and Babalola [34] studied the weight content on the corrosion resistance and effects of alumina nano-particle size of AA1070 aluminium in sulphate/chloride. The study of machinability of pure Al and 12% silicon alloys was investigated against uncoated carbide and coated carbide tools by Roy et al. [35]. Their test results disclose that the affinity of aluminium towards chemical inertness of diamond was solely responsible for outdoing an uncoated tool along with other hard coating tools like TiN, TiC and Al_2O_3, TiB_2.

From the past literature, it was found that very few studies have been reported in Al-SiCp nano particle nano-composite metal matrix with machining of coated carbide tool. So the present research work concentrates on machining of aluminium and silicon carbide nano composite with coated carbide tool.

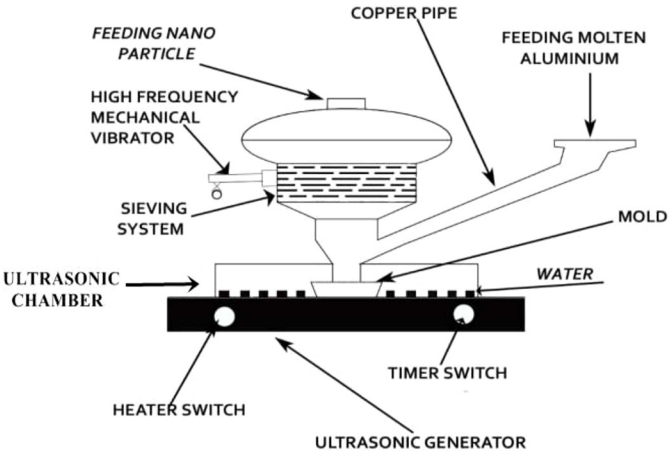

Fig. 1. Schematic diagram of setup for Al-SiCp sample preparation.

3 Experimental procedure of Al-SiCp workpiece

In this process, aluminium is treated as matrix and Silicon Carbide acts as a reinforcement. Aluminium powder is mixed with Silicon carbide nano particles with three different weight percentages of 1, 1.5 and 2 to form Al-SiC nano composites. First of all, synthesis of Al-SiCp nano composite work-piece is carried out. The nano particle SiCp is supplied to the feeder which passes through various sieving system. The molten metal of aluminium is poured at the same time into the pouring pipe. High frequency mechanical vibrator is then made to start. As a result, the requisite size of SiCp nano particles is formed and the mixture of Al and SiCp are moved to the steel through the helical passage as shown in Figure 1.

Ultrasonic waves of 35 KHz are generated by the ultrasonicator. Sufficient amount of water is kept all around the steel die so that ultrasonic waves transmission can take place from the sides of the ultrasonic chamber to form cast ingot of nano composite.

Table 1. Tensile test of Al-SiCp MMNC.

Sl. No.	Al-SiCp wt.%	% of Elongation of Al-SiCp	Ultimate tensile strength (Pa)
1	1	5.15	109.33
2	1.5	4.23	140.72
3	2	3.70	148.96

3.1 Characterization of work piece material (Al-SiCp)

Characterization of a material gives the information of different properties. These properties include physical property, mechanical property, electrical property, chemical property microstructural property and many more. These property evaluations decide the further usefulness of the product. It is therefore very much necessary to evaluate the properties before going for using it for some specific purpose.

3.1.1 Tensile test of workpiece material (Al-SiCp)

The tensile test is conducted for the specimen that was prepared from the cast ingot of aluminium and silicon carbide nano composite material. Universal testing machine (Instron, 100 KN capacity) is used for tensile test for all the three specimens. Table 1 shows the tensile test of the Al-SiCp metal matrix nano composite for all the three samples. It is observed that the elongation of the material decreases due to higher weight % of SiCp particle in the Al matrix which indicates that the fracture toughness increases with the increase in SiCp % in aluminium. Further, the ultimate tensile strength is higher in specimen 3 due to higher weight % of SiCp particle in the Al matrix.

3.1.2 Vickers's-hardness test of workpiece material (Al-SiCp)

Generally, hardness test is done to know the hardness (solidity/rigidity) of the sample. In the present research, Vickers's hardness test is conducted in HECKERT hardness testing machine. The hardness tester uses the menu interface type structure and has a large screen display LCD. The test is conducted for a load of 25 kg-f and a dwell time of 30 s. The different hardness values are noted for a specimen and their average values are recorded. Figure 2 shows the samples prepared for micro hardness test. Table 2 shows the average Vickers hardness values of the nano composites.

From Table 2 it is observed that the micro hardness value of sample 3 is higher than sample 1 and 2 due to higher wt.% of silicon carbide. Hence, it is concluded that with the increased wt. percentage of silicon carbide, the hardness value of the nano composite material also increases.

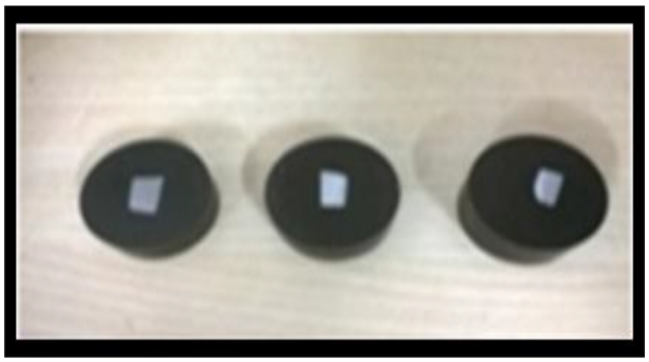

Fig. 2. Prepared Al-SiCp specimen for Vickers's hardness test.

Table 2. Vickers's hardness test of nano composites.

Different specimens	Vickers's hardness values
[Al+SiCp1 wt.%]	54.423
[Al+SiCp1.5 wt.%]	64.926
[Al+SiCp2 wt.%]	68.006

3.1.3 Microstructural analysis of Al-SiCp metal matrix nano composite

The microstructural analysis i.e. EDS and Optical microscopy has been carried out for the Al-SiCp metal matrix nano composite.

3.1.3.1 EDS (Energy Dispersive Spectroscopy)

It is a method which is used to analyze the chemical characterization of Al-SiCp nano composite material. The Al-SiCp metal matrix nano composite is viewed under SEM. A particular portion of the section is magnified at 100 µm zoom and EDAX analysis is performed on Al + SiCp (2 wt.%) to know the chemical characterization of the sample. 2 wt.% sample is chosen as adding more than 2 wt.% of SiCp in aluminium metal matrix composite can cause high viscosity and it will not be convenient to mix with SiCp nano particles uniformly. Figure 3 shows the EDS analysis of Al-SiCp MMNC of 2 wt.%.

Table 3 shows the atomic % and wt.% of Al-SiCp MMNC of 2 wt.% obtained from EDS analysis. From the table it is observed that carbon, silicon and aluminium are present in the *K*th shell. The atomic % of carbon is found to be 76.32% whereas the atomic % of Si and Al are found to be 1.22% and 21.32% respectively. The presence of carbon content might be due to the interaction of tool (low speed abrasive cutter) with the workpiece. Further, the presence of carbon content might be due to the casting pot during the preparation of MMNC. Further, diamond polishing was applied to the workpiece prior to the EDAX process due to which the carbon content might be present.

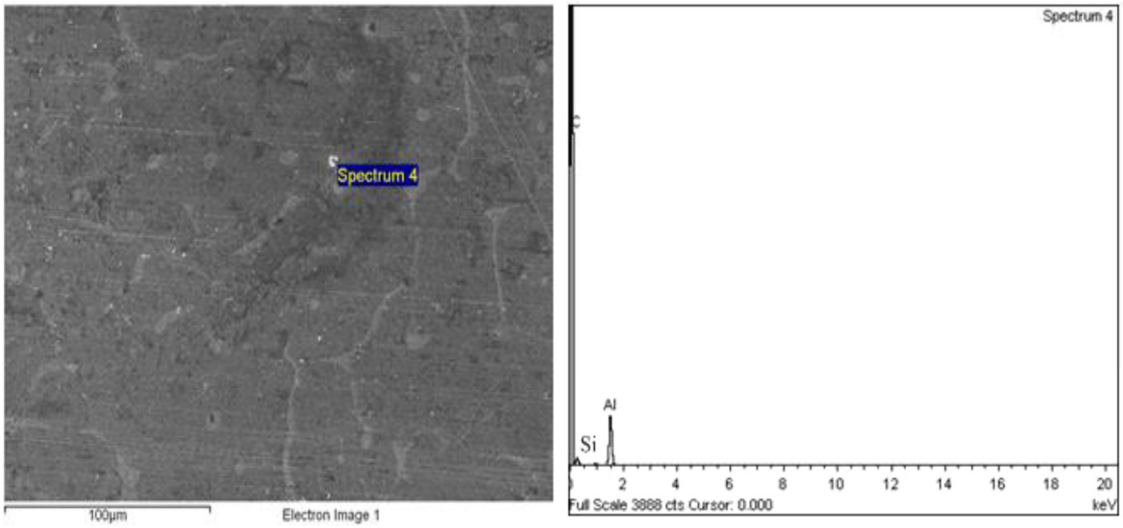

Fig. 3. EDS analysis of Al-SiCp workpiece of 2 wt.%.

Table 3. Atomic % and weight % of Al-SiCp MMNC of 2 wt.% obtained from EDS analysis.

Ingredient	App conc.	Intensity	wt.%	Wt.% sigma	Atomic%
Carbon	0.03	0.4446	58.79	7.15	76.32
Oxygen	0.01	1.3042	2.04	0.85	1.14
Silicon	0.02	0.5032	0.93	1.67	1.22
Aluminium	0.04	1.2607	38.24	2.15	21.32
Totals			100		100

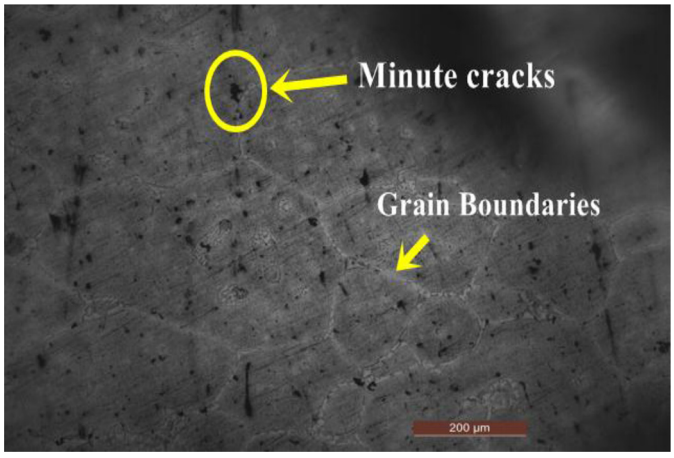

Fig. 4. Optical microscopic view of sample (Al+ SiCp 2 wt.%).

3.1.3.2 Optical microscopy of Al-SiCp workpiece

The image of sample 3 is visualized under optical microscope. Figure 4 shows the optical images of 2 wt.% sample of Al-SiCp nano particle composites at 200 µm optical zoom. It is observed from the figure that grain boundaries and minute cracks are formed on Al + SiCp nano composite material after the machining process. The formation of cracks might be due to the high heat and temperature during the casting operation and the formation of grain boundaries might be due to the effect of mechanical properties of Al and silicon carbide and etching of metal matrix nano composites.

3.2 Methods and preparation of coated tool

Aluminium and silicon carbide nano particle nano composite of a rounded bar casting ingot of 44 mm diameter and 65 mm long is used for hard turning under dry cutting environment on CNC lathe as shown in Figure 5. Coated tool 12040822TN 6010 is used as the tool material whereas Aluminium-Silicon carbide nano composite material is used as the workpiece. The machining is carried out on sample 3 (2 wt.%) as adding more than 2 wt.% of SiCp in aluminium metal matrix composite can cause high viscosity and it will not be convenient to mix with SiCp nano particles uniformly. Further, tensile strength and hardness of sample 3 is higher than sample 1 and 2. So 2 wt.% sample (Sample 3) is chosen for the experimentation. The tool insert is mounted on the tool holder. Three process parameters are selected at four different levels using Taguchi L_{16} orthogonal array. Flank wear (VBc) and average surface roughness (R_a) of cutting inserts are chosen as the response parameters. The design

Fig. 5. Machining operation of coated tool in CNC lathe machine.

Table 4. Input parameters, ranges and levels for the design of experiments.

Parameters/Levels	Units	I	II	III	IV
Cutting speed (v)	(m/min)	70	140	210	280
Feed (f)	(mm/rev)	0.05	0.1	0.15	0.2
Depth of cut (d)	(mm)	0.1	0.2	0.3	0.4

of experiment is created using MINITAB 17 software. A fixed machining length of 100 mm has been set for each experimental run. Prior to the experiment, rust skin layers are removed by conducting some initial cut. New cutting edge is used at each experimental run. Control limit for maximum flank wear (0.3 mm) and surface roughness (1.6 μm) has been set for hard machining. After the completion of experiment, the chips samples are collected for the microstructural study. Table 4 shows the process parameters, levels and ranges selected for the design of experiments. The input parameters and ranges are selected according to their machining limits and past literature survey. The cutting conditions for hard turning are depicted in Table 5.

3.2.1 Determination of flank wear and surface roughness

Surface roughness defines the quality of the surface after machining. Larger deviations cause higher surface roughness whereas smaller deviations cause smoother surface. Surface roughness is measured by Talysurf instrument. It is denoted by Ra and is measured in micrometre (μm). The surface roughness (Ra) of the MMC is measured after the machining operation.

Similarly, *Flank wear occurs* at the tool flanks when it contacts with the finished surface due to adhesion and abrasion wear. It is the gradual failure of the cutting tools

Table 5. Cutting conditions for hard turning.

Cutting conditions	
Workpiece	Al-SiCp metal matrix
Cutting environment	Dry
Hardness	55±1 HRC
Tool holder	PCLNR2525M12
Cutting tool insert geometry	CNMG 12040822 for carbide
Overhang length	30 mm
Cutting inserts	Coated carbide, Insert CNMG 12040822 TN 6010

in which the tool portion with the finished part erodes. It is denoted by VBc. It is measured in terms of mm.

Table 6 shows the Taguchi L_{16} orthogonal array designed for the experiment and values obtained at different experimental runs.

4 Multi objective optimization of response parameters

Optimization is a technique to identify and obtain the best possible outcomes from a given set of results. Pearson first introduced the *Principal Component Analysis* (PCA) and later it was developed by Hotelling. Principal Component Analysis is a multivariate technique in which new uncorrelated variables are formed through a linear composite of the original variables. The maximum number of new variables formed is equivalent to the number of original variables.

In the present paper this technique has been used to optimize the output responses of the input parameters. The purpose of the optimization is to minimize the flank wear and surface roughness.

4.1 Steps for calculating principal component analysis (PCA)

It is a statistical procedure which converts a number of observations of possibly correlated variables into a set of values using an orthogonal transformation called as *Principal Components*. The steps involved in the PCA are

4.1.1 Normalization of process parameters

The multi objective optimization is conducted by using the Principal Component Analysis where the two outputs (Ra and VBc) are combined to get a single value (CQL) in order to get an optimal combination of the setting.

The experimental data is initially normalized considering "lower the better" criteria i.e. Xi*(k). Xi*(k) = [min Yi (k)/Yi (k)] where Xi*(k) is the normalized data of the *k*th element in the *i*th sequence.

Table 6. Input parameters and responses obtained at different runs.

	Process parameters			Response parameters	
Run No.	Depth of cut (d) mm	Feed (f) mm/rev	Cutting speed (v) m/min	R_a (μm)	VB_C (mm)
1	0.1	0.05	70	0.47	0.097
2	0.1	0.10	140	0.50	0.108
3	0.1	0.15	210	0.58	0.131
4	0.1	0.20	280	0.75	0.150
5	0.2	0.05	140	0.52	0.109
6	0.2	0.10	70	0.61	0.111
7	0.2	0.15	280	0.70	0.147
8	0.2	0.20	210	0.78	0.141
9	0.3	0.05	210	0.53	0.134
10	0.3	0.10	280	0.74	0.158
11	0.3	0.15	70	0.91	0.124
12	0.3	0.20	140	1.04	0.134
13	0.4	0.05	280	0.76	0.172
14	0.4	0.10	210	0.91	0.137
15	0.4	0.15	140	1.01	0.129
16	0.4	0.20	70	1.37	0.133

4.1.2 Finding out the Pearson's correlation coefficient (P)

If P value is zero, PCA can't be applied. The next step is checking for the correlations and finding out Pearson's correlation coefficient (P). If P value is 0, PCA can't be applied. All the responses are correlated to each other due to the correlation coefficients of non-zero value. Principal component analysis (Eigen vector, Eigen value, cumulative accountability proportion and accountability proportion) are applied in order to remove the response correlation.

4.1.3 Finding out the individual PCA

4.1.3.1 Calculation of Multiple Performance Index (MPI)

If MPI is negative, CQL will be considered into account.

4.1.3.2 Calculation of Combined Quality Loss (CQL)

Table 7 shows the optimization of response parameters of Taguchi L_{16} orthogonal array using PCA. Table 8 shows the response table of mean signal to noise ratio of CQL. Table 9 shows the results of confirmation experiment for multi-responses.

Equation (1) shows the equation of predicted values of S/N ratio.

$$\overline{Y} = Y_m + \sum_{i=0}^{1} (\overline{Y}_i - Y_m) \quad (1)$$

where γ_m is the mean signal to noise ratio of CQL, $\overline{Y}_i$ is the mean signal to noise ratio at optimal level.

From Table 8, it is noticed that feed (f), depth of cut (d) and cutting speed (v) is found to be highest at Level 1, 1 and 2 of the settings respectively (**0.1-0.05-140**) which is not present in the experimental run L_{16}. Therefore, again the experiment has been carried out by taking $d = 0.1$ mm, $f = 0.05$ mm/rev and $v = 140$ m/min and required Ra and VBc has been found out.

From Table 9 it is noticed that there is a significant improvement of signal-to-noise ratio in confirmation run and found to be 6.488 dB. Surface roughness (Ra) is found

Table 7. Optimization of response parameters using PCA.

Run number	MPI	CQL	S/N Ratio of CQL
Ideal value	1.1736	0.0000	–
1	1.1736	0.0000	–
2	1.0736	0.1000	19.999
3	0.9016	0.2720	11.309
4	0.7496	0.4240	7.452
5	1.0509	0.1227	18.223
6	0.9774	0.1963	14.143
7	0.7798	0.3938	8.095
8	0.7675	0.4061	7.828
9	0.9256	0.2480	12.110
10	0.7304	0.4432	7.068
11	0.7941	0.3796	8.414
12	0.7227	0.4510	6.917
13	0.6873	0.4863	6.261
14	0.7416	0.4320	7.289
15	0.7488	0.4249	7.435
16	0.6757	0.4979	6.057

Table 8. Response table of mean signal to noise ratio of CQL.

Symbol	Input parameters	Mean S/N ratio				Max-Min	Rank
		Level-I	Level-II	Level-III	Level-IV		
d	Depth of cut	**12.920**	12.072	8.627	6.761	6.160	1
f	Feed	**12.198**	12.125	8.813	7.064	5.134	3
v	Cutting speed	9.538	**13.144**	9.634	7.219	5.925	2

Table 9. Results of confirmation experiment for multi-responses.

	Initial input parameters	Optimal input parameters	
		Predicted	Experiment
Level	d2-f3-v4	d1-f1-v2	d1-f1-v2
Ra	0.70		0.48
VBc	0.147		0.101
S/N Ratio of CQL	8.095	20.8243	14.583
Improvement of S/N ratio of CQL = 6.488.			

Table 10. Analysis of Variance for VBc.

Source	DF	Seq SS	Adj SS	Adj MS	F	P	% Contribution	Remarks
d	3	0.0011237	0.0010807	0.0003602	7.31	0.028	19.427	Significant
f	3	0.0003397	0.0003107	0.0001036	2.10	0.219	5.873	Insignificant
v	4	0.0040746	0.0040746	0.0010186	20.66	0.003	70.446	Significant
Error	5	0.0002465	0.0002465	0.0000493			4.261	
Total	15	0.0057844					100	
R-Sq = 95.74% R-Sq(adj) = 87.22%.								

Table 11. Analysis of variance for Ra.

Source	DF	Seq SS	Adj SS	Adj MS	F	P	% Contribution	Remarks
d	3	0.446225	0.438956	0.146319	46.16	0.000	50.731	Significant
f	3	0.372875	0.372250	0.124083	39.14	0.001	42.392	Significant
v	4	0.044625	0.044625	0.011156	3.52	0.100	5.073	Insignificant
Error	5	0.015850	0.015850	0.003170			1.802	
Total	15	0.879575					100	
R-Sq = 98.20% R-Sq(adj) = 94.59%.								

to be decreased 1.458 times in confirmation run during turning. Similarly, VBc is found to be decreased 1.455 times in confirmation run during turning.

5 Results and discussion

Analysis of variance or ANOVA are used to determine the most influencing parameters in affecting the output responses. P determines the probability value. If the value of P is less than 0.05, the factor is said to be significant. Similarly, the main effect plots are used to analyse the effect of input parameters and output responses. *Mean* in the main effect plot signifies the mean/average value of the individual responses of the respective input parameters.

5.1 ANOVA and main effect plot for flank wear and surface roughness

Tables 10 and 11 show the ANOVA for VBc and Ra respectively. Similarly, Figures 6 and 7 depict the main

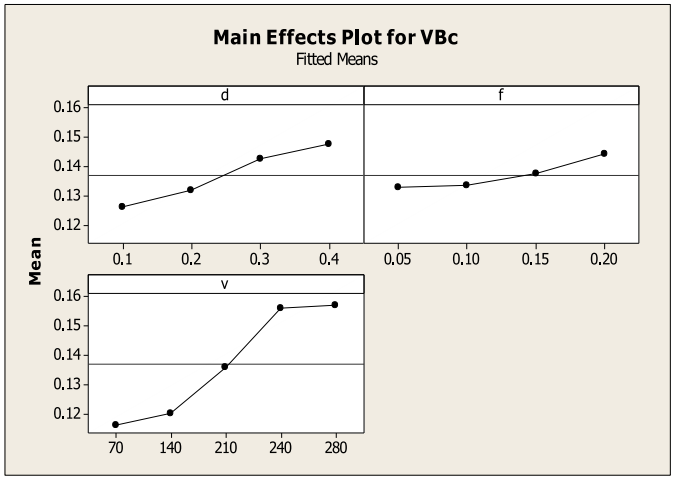

Fig. 6. Main effect plot for VBc.

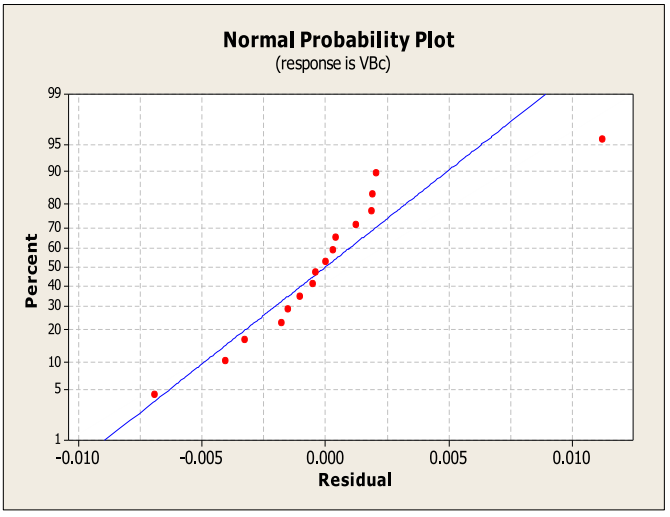

Fig. 8. Normal Probability plot of coated VBc.

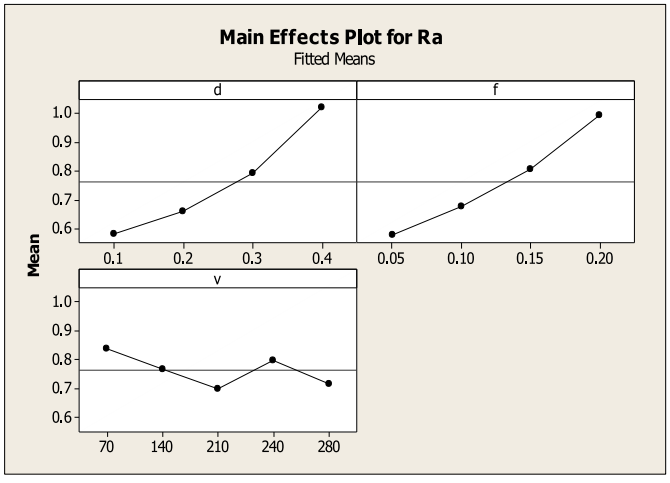

Fig. 7. Main effect plot for Ra.

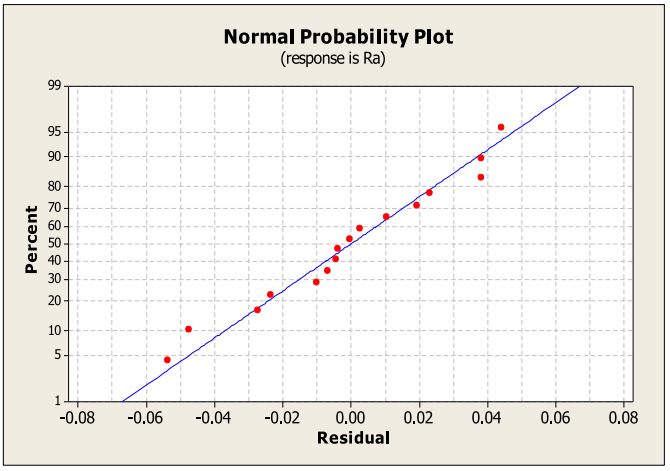

Fig. 9. Normal Probability plot of coated Ra.

effect plot for VBc and Ra respectively. From the ANOVA table it is concluded that *depth of cut (d)* and *speed (v)* are the two most important factors influencing the responses for VBc. Similarly, *depth of cut* and *feed* are found to be the most significant factors affecting the responses for Ra from the ANOVA table.

From Figure 6, it is cleared that the flank wear (VBc) growth increases with the rise of feed, speed and depth of cut. Further, it is found that the rise of flank wear is at a slower rate due to the increase of feed. The increase of depth of cut and cutting speed are predominant parameters and the flank wear is sharply increased to its maximum value of 240 m/min. So from the above figure, cutting speed and depth of cut are the two important and crucial parameters for flank wear whereas feed does not indicate any statistical significance on flank wear for coated carbide insert.

From Figure 7, it is concluded that the surface roughness (Ra) increases with the increase of feed as well as depth of cut, but it decreases highly at cutting speed 280 m/min. The surface roughness decreases due to the increase of speed from 70–210 m/min and it slightly increases during 210–240 m/min and then decreases from 240 to 280 m/min. So from the above discussion it is finalized that feed as well as depth of cut are the two significant factors to control the surface roughness.

5.2 Normal probability plot

The normal probability plot is used to classify deviations from normality. The point closet to the normal line satisfies the fitness of the model. Figures 8 and 9 shows the normal probability plot of VBc and Ra during machining by coated carbide insert. From Figures 8 and 9, it is noticed that all the 16 points lies close to the normal line which confirms the normal distribution of the data sets. The normal probability plot also shows a good sign of the model as all the 16 points lies closer to the normal line.

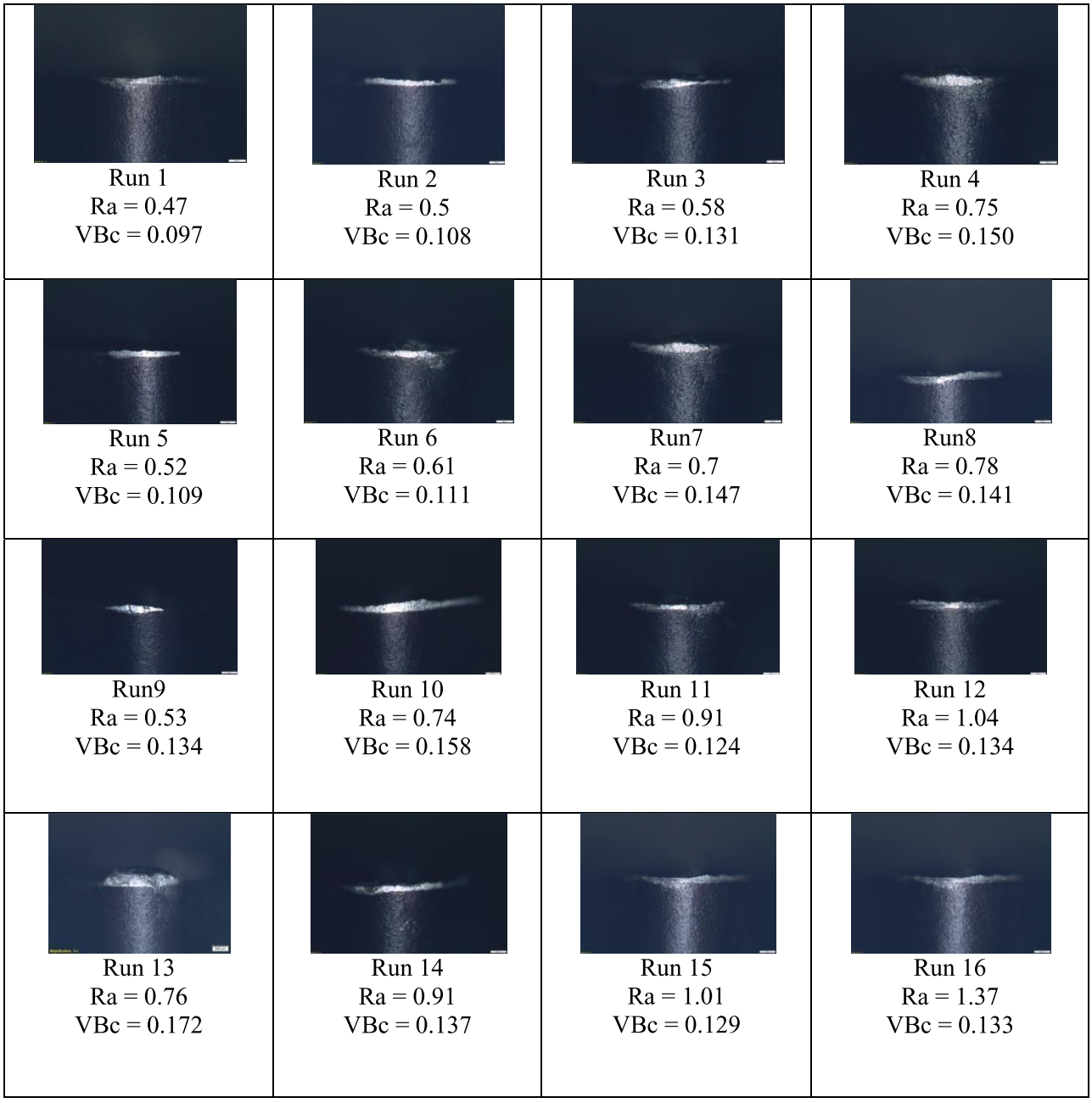

Fig. 10. Optical image analyses of coated tool during machining of Al-SiCp matrix at different runs.

5.3 Optical image analysis of coated Al-SiCp matrix

Figure 10 shows the optical image analysis while machining of coated Al-SiCp matrix at different runs. Tool wear is characterized by diffusion and abrasion. The interface temperature quickly rises at higher cutting speeds leading to the softening of the cutting tool inserts due to the generation of heat. High mechanical loading along with the friction at the interfaces on the cutting edge leads to abrasion.

From the obtained cutting parametric ranges, different modes of cutting tool failure and wear mechanisms can be observed during experimentation. Some cutting tool elements are removed away with continuous rubbing. It is observed that coated carbide inserts suffered from higher flank wear (Run 13) and excessive surface roughness (Run 16). Abrasives scars at flank surface, failure of the tool tip, adhesion of metal and deformation of chipping and cutting edge can be clearly observed from the captured figures. Catastrophic failure is marked at the cutting edge, thus owing to mechanical fatigue. The flank face suffers accelerated wear for coated carbide insert due to absence of hot hardness property. Fracture in the tool tip is also observed and is due to the high shear stress generated by gradual increase in the temperature gradient for coated carbide insert. At high feed rate and cutting speed, some

plastic deformation can be observed on the cutting edge. Therefore, chipping is the major source of the cutting tool failure that is noticed in the studied range and is due to the inadequate strength to sustain high stress at elevated parametric conditions.

5.4 Analysis of flank wear measurement of coated tool

Various types of tool wear for multilayer coated carbide cutting tool has been investigated by turning test and their captured images are shown in Figure 10. From Table 6, it has been confirmed that when the depth of cut becomes 0.1 mm for Run 1 and 2, flank wear (VBc) increases from 0.097 to 0.108 mm by increasing the cutting speed from 70 to 140 m/min and feed 0.05–0.10 mm/rev. Again at the same depth of cut (0.1 mm), feed (0.15–0.2 mm/rev) for run 3 and 4, the flank wear increases from 0.131 mm to 0.150 mm with increase in the speed from 210 to 280 mm/min. But it is found that in each run, the tool wear lies within the permissible wear range of 0.3 mm. It is also noticed that at higher cutting speed i.e. 280 m/min for run number 4, 7, 10 and 13, the flank wear also lies within the permissible limit of 0.3 mm. However, it is observed that VBc increases for run no 4, 10 and 13 and slightly decreases for run no. 7. It is due to the fact that at run no. 4, feed is highest (0.20 mm/rev) while at run no. 7 feed is lowest (0.15 mm/rev). Further it is concluded that feed has also significant contribution on flank wear. Again, as feed is less in case of run no. 7 as compared to run no. 4, so surface roughness decreases at run no. 7.

From the pictures of the cutting edges (Fig. 10), it is concluded that at maximum speed, the wear of the tool takes place with minor chipping. This phenomenon might be due to thermo-mechanical loading on the cutting edges of the tool. Further, at higher cutting speed, high temperature generates which leads to tool wear. So from the above discussion it has been confirmed that the coated carbide cutting inserts are suitable for machining process giving better surface finish and less flank wear under any dry environmental machining conditions. The improved result of multilayer coated carbide tool indicates that maximum heat generated during the machining is absorbed by the workpiece due to the thermal barriers of the cutting tool. This phenomenon also prevents the flank wear growth of the cutting tool during the machining operation.

6 Conclusions

Characterization and machining study of Al-SiCp nano composites were discussed. It was observed that the ultimate tensile strength of the material is 148.06 Pa and percentage of elongation is 3.7% which was quite satisfactory for industrial and automobile applications. Further, from the Vickers hardness test it was concluded that the nano composite material is suitable for various machining operations. The microstructural analysis shows that the material is quite suitable for sustaining high temperature and heat for its machining process. Different parameters like speed, feed and depth of cut were optimized by using PCA and optimal combinations were obtained ($d = 0.1$ mm, $f = 0.05$ mm/rev and $v = 140$ m/min) which shows the feasibility of Al-SiCp nano composite material. ANOVA results shows that the most significant factors affecting the responses i.e. surface roughness of workpiece (Ra) and flank wear of tool (VBc) are quite good for various applications. Finally, the optical image analysis of the coated carbide tool indicates its wear capability and resistivity of Al-SiCp due to high temperature gradient.

7 Scope of future work

Some of the scopes for the future works are listed as below.

- Volume fraction/weight fraction of SiC_p reinforcements and particle sizes can be varied to find out the best strength and quality nano composite.
- The effect of ultrasonically assisted casting on the dimensions of the cast ingot can be studied and the best possible size of the cast product can be achieved.
- Flexural strength and the fatigue strength can be evaluated for the developed nano composites.
- Weldability property of the developed nano composite can be studied with TIG, MIG and FSW. This can help in providing in-depth information about the joining of the developed composites.
- Flank wear (tool) and surface roughness of Al-SiC_p nano composite can be compared with wiper geometry coated carbide insert with same cutting conditions.
- Performance of multilayer coated and uncoated carbide tool under spray impingement cooling environment and MQL environment in turning can be investigated.
- Some forming operation like rolling and extrusion can be carried out with the developed composite for studying the formability.

References

[1] S.S. Kumar, M. Uthayakumar, S.T. Kumaran, P. Parameswaran, E. Mohandas, Electrical Discharge Machining of Al (6351)-5% SiC-10% B_4C hybrid composite: a grey relational approach, Int. J. Mater. Product Technol. **53**, 86–97 (2014)

[2] S. Gatea, H. Ou, G. McCartney, Deformation and fracture characteristics of Al6092/SiC/17.5p metal matrix composite sheets due to heat treatments, Mater. Charact. **142**, 365–376 (2018)

[3] H. Kala, K.K.S. Mer, S. Kumar, A review on mechanical and tribological behaviors of stir cast aluminum matrix composites, Mater. Sci. **6**, 1951–1960 (2014)

[4] N. Singh, I.U.H. Mir, A. Raina, A. Anand, V. Kumar, S.M. Sharma, Synthesis and tribological investigation of Al-SiC based nano hybrid composite, Alexandria Eng. **42**, 67–73 (2016)

[5] L. Kollo, M. Leparoux, C.R. Bradbury, C. Jaggi, E.C. Morelli, M.R. Arbaizar, Investigation of planetary milling for nano-silicon carbide reinforced aluminium metal matrix composites, J. Alloys Comp. **489**, 394–400 (2010)

[6] S. Gopalakannan, T. Senthilvelan, Application of response surface method on machining of Al-SiC nano-composites, Measurement **46**, 2705–2715 (2013)

[7] A. Mazahery, M.O. Shabani, Nano-sized silicon carbide reinforced commercial casting aluminum alloy matrix: experimental and novel modeling evaluation, Powder Technol. **217**, 558–565 (2012)
[8] S. Li, Y. Su, X. Zhu, H. Jin, Q. Ouyang, D. Zhang, Enhanced mechanical behavior and fabrication of silicon carbide particles covered by in-situ carbon nanotube reinforced 6061 aluminum matrix composites, Mater. Des. **107**, 130–138 (2016)
[9] N. Chawla, Y.L. Shen, Mechanical behavior of particle reinforced metal matrix composites, Adv. Eng. Mater. **3**, 357–370 (2001)
[10] M. Dhanashekar, V.S. Senthil Kumar, Squeeze casting of aluminium metal matrix composites − an overview, Eng. Mater. **97**, 412–420 (2014)
[11] K.R. Padmavathi, R. Ramakrishnan, Tribological behaviour of aluminium hybrid metal matrix composite, Eng. Mater. **97**, 660–667 (2014)
[12] D.K. Koli, G. Agnihotri, R. Purohit, A review on properties, behaviour and processing methods for Al-Nano Al_2O_3 composites, Mater. Sci. **6**, 567–589 (2014)
[13] S. Divagar, M. Vigneshwar, S.T. Selvamani, Impacts of nano particles on fatigue strength of aluminum based metal matrix composites for aerospace, Mater. Today **3**, 3734–3739 (2016)
[14] K.J. Lijay, J.D.R. Selvam, I. Dinaharan, S.J. Vijay, Microstructure and mechanical properties characterization of AA6061/TiC aluminum matrix composites synthesized by in situ reaction of silicon carbide and potassium fluotitanate, Trans. Nonferrous Metals Soc. China **26**, 1791–1800 (2016)
[15] A. Radha, K.R. Vijayakumar, An investigation of mechanical and wear properties of AA6061 reinforced with silicon carbide and graphene nano particles-particulate composites, Mater. Today **3**, 2247–2253 (2016)
[16] M.T. Sijo, K.R. Jayadevan, Analysis of stir cast aluminium silicon carbide metal matrix composite: a comprehensive review, Technology **24**, 379–385 (2016)
[17] D. Dhaneswara, A.Z. Syahrial, M.T. Ayman, Mechanical properties of nano SiC-reinforced aluminum A356 with Sr modifier fabricated by stir casting method, Proc. Eng. **216**, 43–50 (2017)
[18] I. Manivannan, S. Ranganathan, S. Gopalakannan, S. Suresh, K. Nagakarthigan, R. Jubendradass, Tribological and surface behavior of silicon carbide reinforced aluminum matrix nanocomposite, Surf. Interfaces **8**, 127–136 (2017)
[19] A. PrasadReddy, P. VamsiKrishna, R.N. Rao, N.V. Murthy, Silicon carbide reinforced aluminium metal matrix nano composites − a review, Mater. Today **4**, 3959–3971 (2017)
[20] R.S. Rana, R. Purohit, P.M. Mishra, P. Sahu, S. Dwivedi, Optimization of mechanical properties of AA 5083 nano SiC composites using design of experiment technique, Mater. Today **4**, 3882–3890 (2017)
[21] M. Razavi, A.R. Farajipour, M. Zakeri, M.R. Rahimipour, A.R. Firouzbakht, Production of Al_2O_3-SiC nano-composites by spark plasma sintering, Surf. Rev. Lett. **56**, 186–194 (2017)
[22] A.M. Davidson, D. Regener, A comparison of aluminium-based metal-matrix composites reinforced with coated and uncoated particulate silicon carbide, Silicon **60**, 865–869 (2000)
[23] S.A. Abolkassem, O.A. Elkady, A.H. Elsayed, W.A. Hussein, H.M. Yehya, Effect of consolidation techniques on the properties of Al matrix composite reinforced with nano Ni-coated SiC, Results Phys. **9**, 1102–1111 (2018)
[24] X. Chen, D. Fu, J. Teng, H. Zhang, Hot deformation behavior and mechanism of hybrid aluminum-matrix composites reinforced with micro-SiC and nano-TiB2, J. Alloys Comp. **753**, 566–575 (2018)
[25] M.A. Xavior, J.P.A. Kumar, Machinability of hybrid metal matrix composite − a review, Proc. Eng. **174**, 1110–1118 (2017)
[26] P. Ramesh, A.A. Raja, R. Ajay, Investigation of wear behavior and mechanical properties of ai-sic metal matrix composites, ARPN J. Eng. Appl. Sci. **11**, 6046–6055 (2016)
[27] V. Mohanavel, K. Rajan, S.S. Kumar, S. Udishkumar, C. Jayasekar, Effect of silicon carbide reinforcement on mechanical and physical properties of aluminum matrix composites, Mater. Today **5**, 2938–2944 (2018)
[28] X. Zhang, S. Li, D. Pan, B. Pan, K. Kondoh, Microstructure and synergistic-strengthening efficiency of CNTs-SiCpdual-nano reinforcements in aluminum matrix composites, Appl. Surf. Sci. **105**, 87–96 (2018)
[29] M. Shukla, S.K. Dhakad, P. Agarwal, M.K. Pradhan, Characteristic behaviour of aluminium metal matrix composites: a review, Mater. Today **5**, 5830–5836 (2018)
[30] G. Somasundaram, S.R. Boopathy, K. Palanikumar, Experimental Investigation on roundness error in friction drilling and mechanical properties of Al/SiCp MMC composites, Mech. Ind. **12**, 445–457 (2011)
[31] S.N. Grigoriev, A.A. Vereshchaka, Methodology of formation of multi-layered coatings for carbide cutting tools, Mech. Ind. **17**, 706–720 (2016)
[32] N. Gangil, S. Maheshwari, A.N. Siddiquee, Influence of tool pin and shoulder geometries on microstructure of friction stir processed AA6063/SiC composites, Mech. Ind. **19**, 211–216 (2019)
[33] R. Behera, S. Kayal, N.R. Mohanta, G. Sutradhar, Study on machinability of aluminium silicon carbide metal matrix composites, Mater. Today **5**, 1–7 (2013)
[34] R.T. Loto, P. Babalola, Effect of alumina nano-particle size and weight content on the corrosion resistance of AA1070 aluminum in chloride/sulphate solution, Res. Phys. **10**, 731–737 (2018)
[35] P. Roy, S.K. Sarangi, A. Ghosh, A.K. Chattopadhyay, Machinability study of pure aluminium and Al − 12% Si alloys against uncoated and coated carbide inserts, Int. J. Refract. Metals Hard Mater. **27**, 535–544 (2009)

Cite this article as: P.K. Swain, K.D. Mohapatra, R. Das, A.K. Sahoo, A. Panda, Experimental investigation into characterization and machining of Al + SiCp nano-composites using coated carbide tool, Mechanics & Industry **21**, 307 (2020)